

# Workshop on top physics at the LC 2017

7-9 junio 2017  
CERN

## NNLO non-resonant and other electroweak corrections at threshold

**Pedro Ruiz-Femenía**

Universidad Autónoma Madrid - IFT

In collaboration with

**M. Beneke, A. Maier and T. Rauh**



Instituto de  
Física  
Teórica  
UAM-CSIC

- I Top-pair production at linear colliders near threshold - QCD and EW corrections
- II Non-resonant contributions @NLO
- III Non-resonant contributions @NNLO
- IV Results
- V Summary

# Top-pair production near threshold

## Future linear colliders (ILC/CLIC)

with  $\sqrt{s} \gtrsim 2m_t \simeq 350$  GeV will produce lots of  $t\bar{t}$  pairs, allowing for a **threshold scan** of the top cross section

↪ **Precise determination** of the top mass  $m_t$ , the width  $\Gamma_t$  and the Yukawa coupling  $\lambda_t$

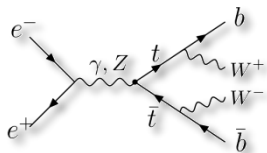
$$\rightarrow \delta m_t \simeq \pm 45 \text{ MeV}$$

↪  $m_t$  is a crucial input for electroweak precision observables!

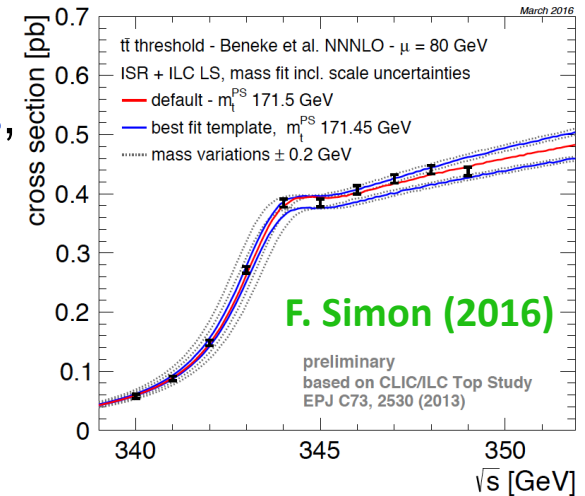
**Requires also precise theoretical prediction**  $\Rightarrow \delta\sigma/\sigma \sim 3\%$

QCD corrections are known up to NNLL/NNNLO, but **electroweak contributions due to top decay** not fully known at NNLO

**Note!** once EW effects are turned on, the **physical final state** is  $W^+W^-b\bar{b}$



$$\Rightarrow \sigma(e^+e^- \rightarrow W^+W^-b\bar{b}) \text{ in the } t\bar{t} \text{ threshold region}$$



Decay  $t \rightarrow bW^+$  with  $\Gamma_t \approx 1.5 \text{ GeV} \gg \Lambda_{\text{QCD}}$   
 $\Rightarrow t\bar{t}$  is **perturbative** at threshold

Top quarks move slowly near threshold:  $v = \sqrt{1 - \frac{4m_t^2}{s}} \sim \alpha_s \ll 1$   
 $\hookrightarrow$  sum  $\left(\frac{\alpha_s}{v}\right)^n$  from “**Coulomb gluons**” to all orders **Fadin, Khoze '87-88**  $\rightarrow$  **NRQCD**  
**Strassler, Peskin '91**

$$R = \frac{\sigma_{t\bar{t}}}{\sigma_{\mu^+\mu^-}} = v \sum_n \left(\frac{\alpha_s}{v}\right)^n \left( \{1\}_{\text{LO}} + \{\alpha_s, v\}_{\text{NLO}} + \{\alpha_s^2, \alpha_s v, v^2\}_{\text{NNLO}} + \dots \right)$$

RG improvement by summing also  $(\alpha_s \ln v)^m$ : **LL, NLL, ...**  $\rightarrow$  **vNRQCD/pNRQCD**

- **NNLO**

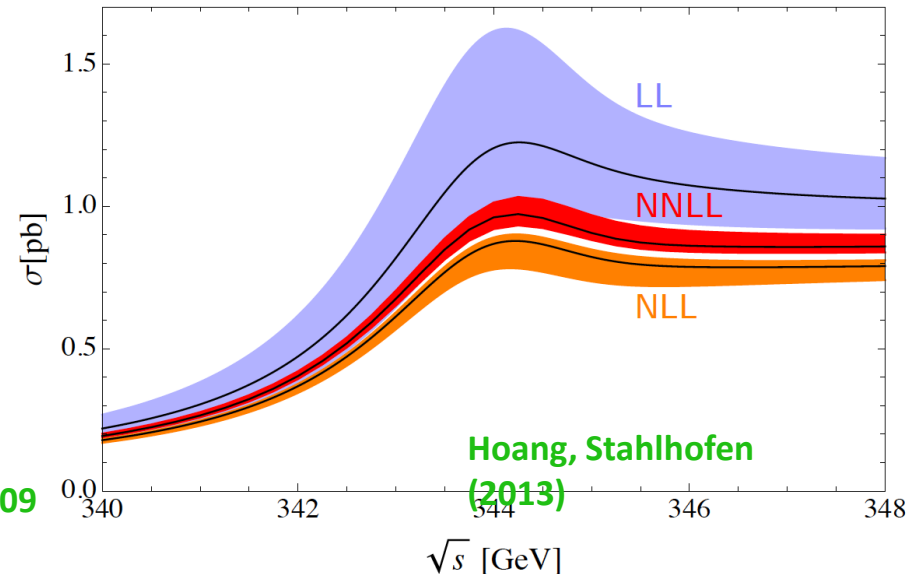
Hoang, Teubner '98-99; Melnikov, Yelkhovsky '98  
 Yakovlev '98; Beneke, Signer, Smirnov '99  
 Nagano, Ota, Sumino '99; Penin, Pivovarov '98-99

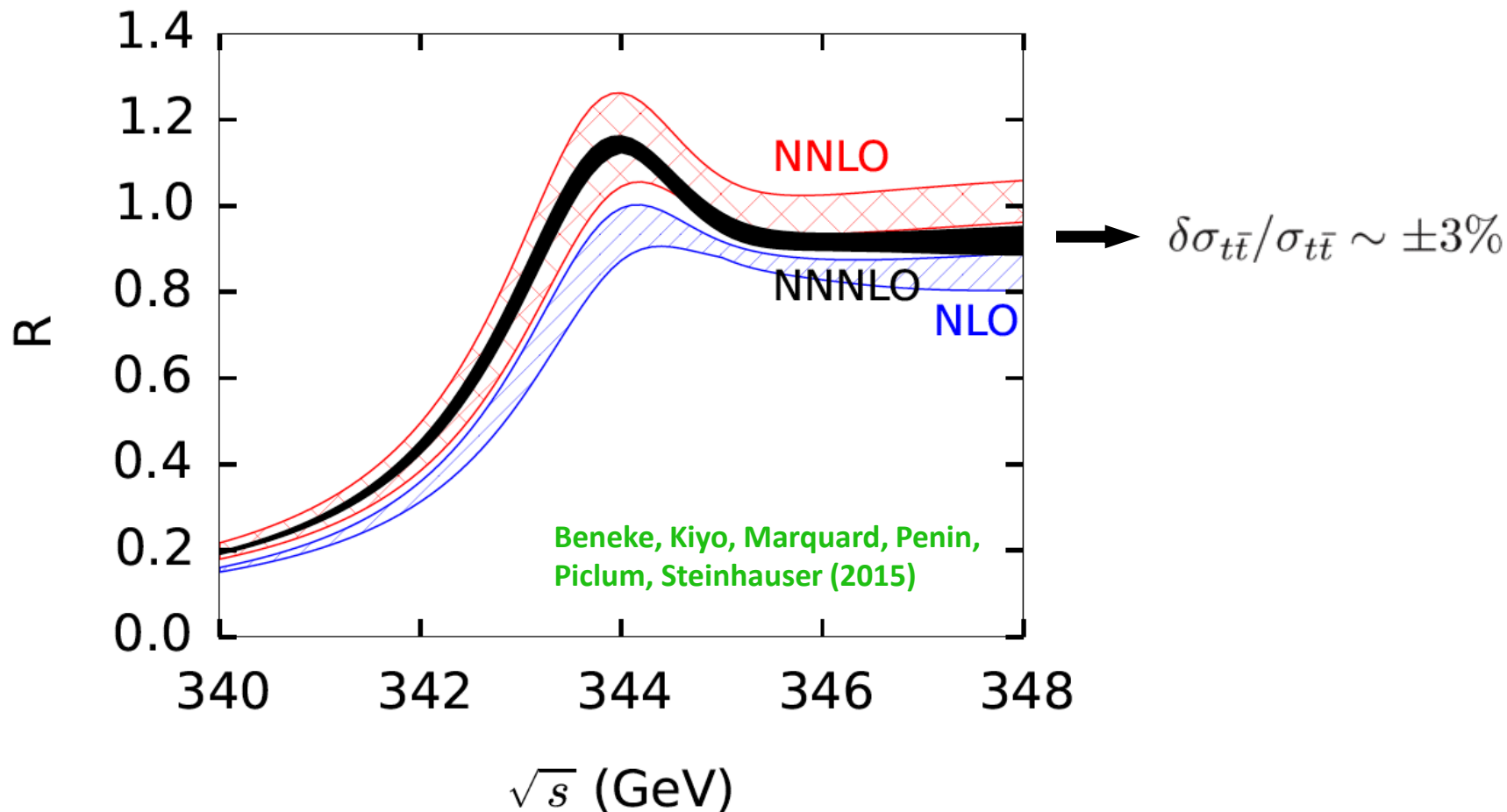
- **NNLL**

Hoang, Manohar, Stewart, Teubner '00-01  
 Hoang '03; Pineda, Signer '06  
 Hoang, Stahlhofen '06-13

- **NNNLO**

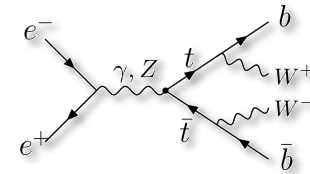
Beneke, Kiyo, Schuller '05-08; Anzai, Kiyo, Sumino '09  
 Smirnov, Smirnov, Steinhauser '08-10  
 Marquard, Piclum, Seidel, Steinhauser '06-14



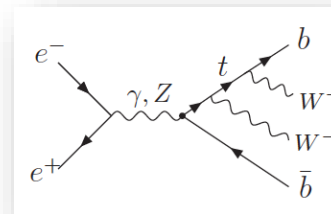


- QQbar\_threshold → [see A. Maier's talk](#)
- EW effects beyond LO and specially non-resonant effects give contributions at the level of the QCD uncertainty

- **Resonant contributions** to  $e^+e^- \rightarrow W^+W^-b\bar{b}$   
top and antitop close to the mass-shell

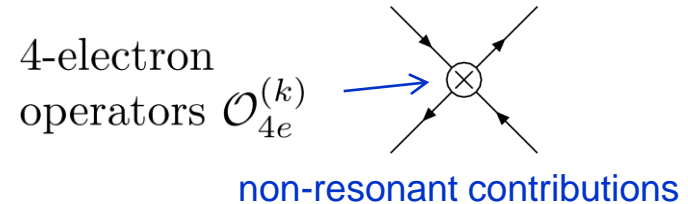
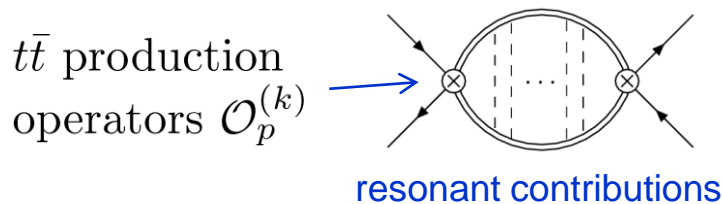


- **Non-resonant (hard) corrections:** account for the production of the  $bW$  pairs by highly virtual tops or diagrams with only one or no top



- **power counting for finite width effects:**  $\frac{\Gamma_t}{m_t} \sim \alpha_{EW} \sim \alpha_s^2 \sim v^2 \ll 1$

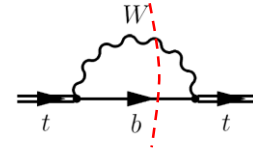
**Effective field theory (EFT)** for pair production of unstable particles near threshold, based on separation of resonant and nonresonant fluctuations



→ Extract cross section for  $e^+e^- \rightarrow W^+W^-b\bar{b}$  from appropriate cuts of the  $e^+e^- \rightarrow e^+e^-$  **forward-scattering amplitude**

## Electroweak effects at LO Fadin, Khoze (1987)

- Replacement rule:  $E = \sqrt{s} - 2m_t \rightarrow E + i\Gamma_t$



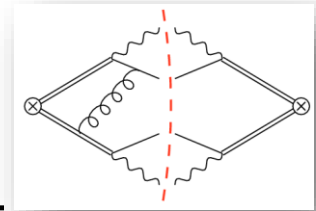
$\Rightarrow$  unstable top propagator

$$\frac{i}{p^0 - \mathbf{p}^2/(2m) + i\Gamma_t/2} \leftarrow \delta\mathcal{L} = \sum_{\mathbf{p}} \psi_{\mathbf{p}}^\dagger i \frac{\Gamma_t}{2} \psi_{\mathbf{p}}$$

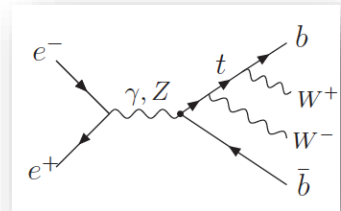
## Electroweak effects at NLO

- Exchange of “Coulomb photon”: trivially extension of QCD corrections

- Gluon exchange involving the bottom quarks in the final state  $\Rightarrow$  these contributions vanish at NLO for the total cross section, Fadin, Khoze, Martin; Melnikov, Yakovlev (1994) also negligible if loose top invariant-mass cuts are applied; remains true at NNLO Hoang, Reisser (2005); Beneke, Jantzen, RF (2010)



- Non-resonant corrections to  $e^+e^- \rightarrow W^+W^-b\bar{b}$  which account for the production of the  $Wb$  pairs by highly virtual tops or with only one or no top

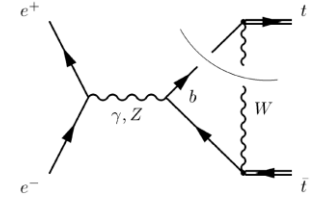


$$\hookrightarrow \Delta\sigma_{\text{non-res}} = \frac{1}{s} \sum_k \text{Im} \left[ C_{4e}^{(k)} \right] \langle e^+e^- | \mathcal{O}_{4e}^{(k)} | e^+e^- \rangle$$

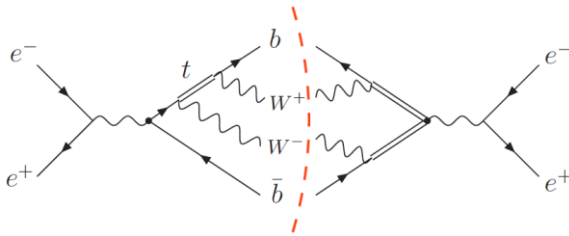
Beneke, Jantzen, RF (2010)

## Electroweak effects at NNLO

- **absorptive parts** in the 1-loop matching coeffs. of the production currents (arising from  $bW$  cuts) Hoang, Reisser (2006)



⇒ reproduce interferences between double and single top (resonant) amplitudes



$$j_v = c_v(\mu) \phi^\dagger \sigma^i \chi$$

$$c_v = 1 + c_v^{(1)} \left( \frac{\alpha_s}{4\pi} \right) + c_v^{(2)} \left( \frac{\alpha_s}{4\pi} \right)^2 + \underbrace{iC_{bW,abs}}_{\text{red circle}} + \underbrace{C_{EW}}_{\text{blue circle}} + \dots$$

- **real part** of hard one-loop EW corrections Guth, Kuhn (1992); Hoang, Reisser (2006)
- **Higgs exchange**, short-distance and potential contributions (N<sup>3</sup>LO) Strassler, Peskin (1991); Beneke, Maier, Piclum, Rauh (2015)
- **initial state QED radiation**: usually taken into account in exp. studies. Produces big effects, analysis at NLL is needed ( $e^\pm$  structure functions) w.i.p
- **NNLO non-resonant** contributions (**gluon corrections** to NLO ones) Partial results available Hoang, Reisser, PRF (2010)  
Jantzen, PRF (2013); PRF (2014) → this talk

## II. Non-resonant NLO contributions

# Non-resonant NLO contributions

Beneke, Jantzen, RF (2010)

⇒ cuts through  $bW^+\bar{t}$  (see diagrams) and  $\bar{b}W^-t$  (not shown) in the 2-loop forward scattering amplitude

- treat loop-momenta as hard:

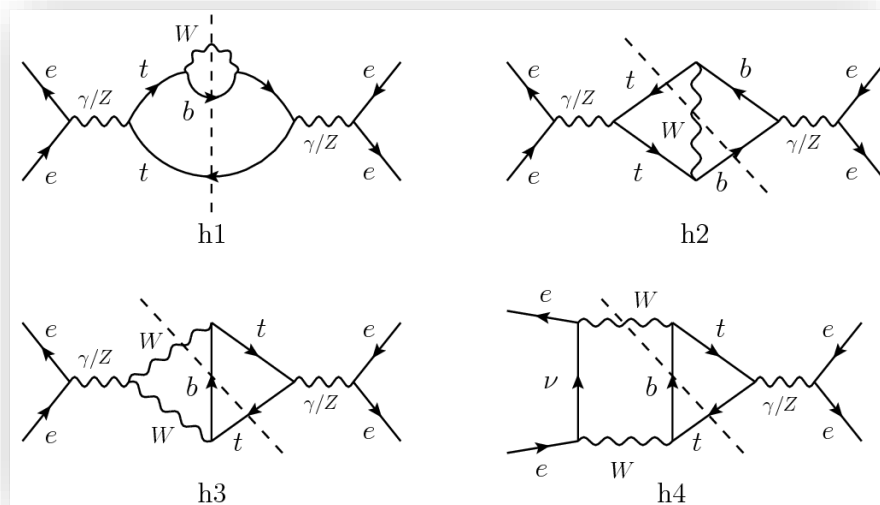
$$p_t^2 - m_t^2 \sim \mathcal{O}(m_t^2) \gg \Sigma(p_t^2) \sim m_t^2 \alpha_{EW}$$

$$\rightarrow \Gamma_t = 0$$

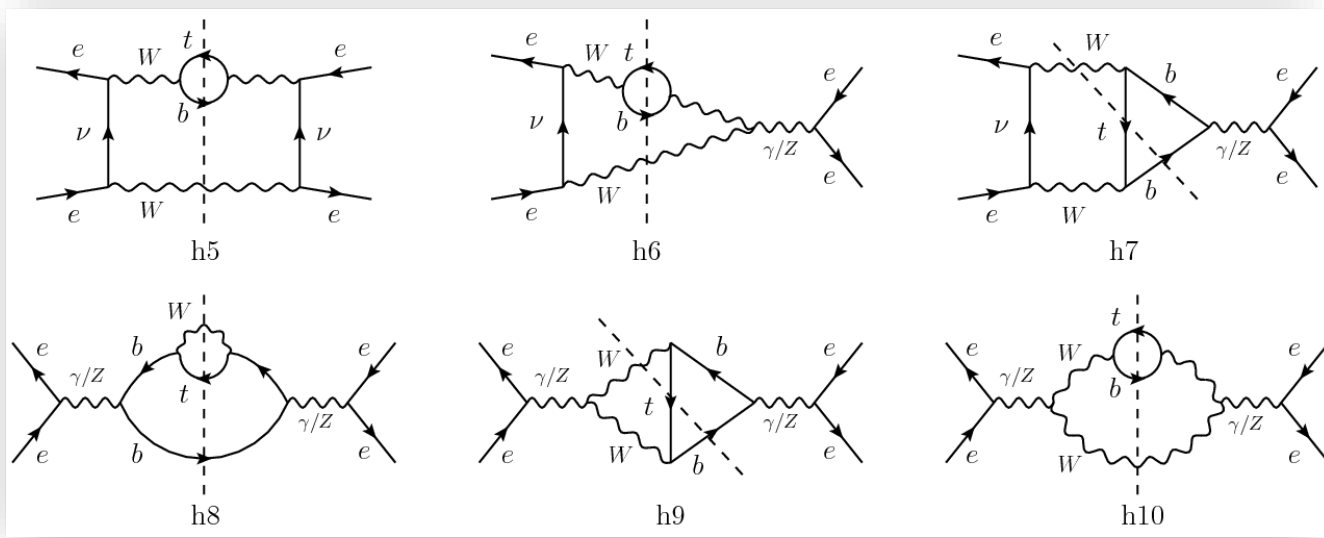
- suppressed w.r.t. LO ( $\sim v$ ) by

$$\alpha_{EW}/v \sim \alpha_s$$

$bW^+$  from highly virtual top



$bW^+$  without intermediate top



In terms of the invariant mass of the  $bW^+$  system,  $p_t^2 = (p_b + p_{W^+})^2$ ,  
 ( $p_t \rightarrow$  also momentum of the top line for h1-h4) diagrams h1-h10 read:

$$\int_{\Delta^2}^{m_t^2} dp_t^2 (m_t^2 - p_t^2)^{1/2-\epsilon} H_i \left( \frac{p_t^2}{m_t^2}, \frac{M_W^2}{m_t^2} \right)$$

with  $\Delta^2 = M_W^2$  for the total cross section

## Applying top invariant-mass cuts

Restrict invariant masses of the reconstructed  $t, \bar{t}$ :  $|\sqrt{p_{t,\bar{t}}^2} - m_t| \leq \Delta M_t$

$\hookrightarrow$  lower integration limit  $\Delta^2 = m_t^2 - \Lambda^2$  where  $\Lambda^2 = (2m_t - \Delta M_t)\Delta M_t$

We focus on **loose cuts** with  $\Lambda^2 \gg m_t \Gamma_t$  (corresponding to  $\Delta M_t \gg \Gamma_t$ )

$\rightsquigarrow$  **cut has no effect in the resonant contributions**

[In contrast: for **tight cuts** with  $\Lambda^2 \sim m_t \Gamma_t$  ( $\Delta M_t \sim \Gamma_t$ ), non-resonant contributions vanish and cuts only affect the resonant contributions]

## III. Non-resonant NNLO contributions

# Finite-width divergences in the resonant contributions

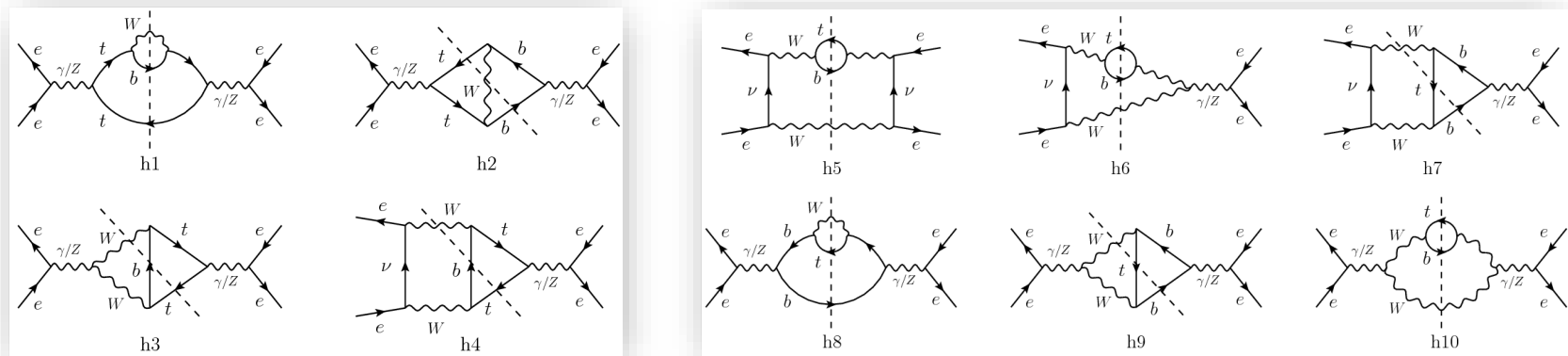
**Resonant contributions** obtained by assuming the top quarks are nearly on-shell (**potential**), but integrated over all momenta

→ uncanceled **UV-singularity** from **hard** momenta:  $\Delta\sigma^{\text{NNLO}} \sim m_t^2 \frac{\alpha_s \Gamma_t}{\epsilon}$

Related to **finite top width** in EFT cut propagator

- for stable top  $\rightarrow \pi \delta(p^0 - \frac{\vec{p}^2}{2m_t})$ ,
- for unstable top  $\rightarrow \frac{\Gamma_t/2}{(p^0 - \vec{p}^2/2m_t)^2 + (\Gamma_t/2)^2}$  Breit-Wigner, UV-behaviour changed!

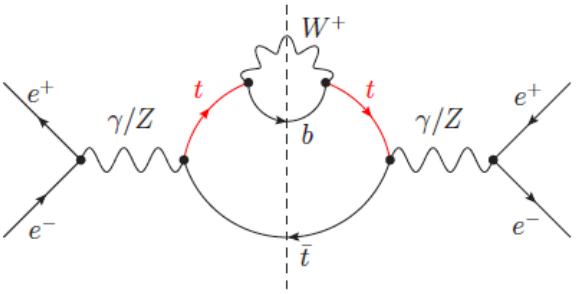
These divergences must **cancel with non-resonant NNLO terms**, which arise from **gluon corrections** to NLO non-resonant diagrams h1-h10



# Endpoint divergences in the non-resonant contributions

Endpoint divergences of the phase-space integration at  $p_t^2 \rightarrow m_t^2$  (because  $\Gamma_t = 0$  here):

**NLO:**

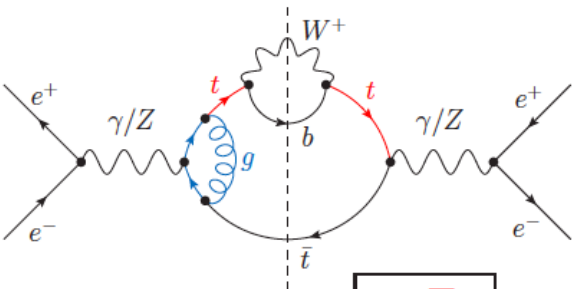


$$\sim \int \frac{dp_t^2}{(m_t^2 - p_t^2)^{n+\epsilon}}$$
 with  $n = \frac{3}{2}, \frac{1}{2}, \dots$

$\hookrightarrow$  endpoint divergence finite in dim. reg.:

$$\int_{m_t^2 - \Lambda^2}^{m_t^2} \frac{dp_t^2}{(m_t^2 - p_t^2)^{\frac{3}{2}+\epsilon}} = -\frac{2}{\Lambda} + \mathcal{O}(\epsilon)$$

**NNLO:**



$$\sim \int \frac{dp_t^2}{(m_t^2 - p_t^2)^{n+a\epsilon}}$$
 with  $n = 2, \frac{3}{2}, \mathbf{1}, \frac{1}{2}, \dots$

$\hookrightarrow$  endpoint divergence  $\propto \boxed{\alpha_s \frac{\Gamma_t}{\epsilon}}$  from  $n = 1$ :

$$\mu^{4\epsilon} \int_{m_t^2 - \Lambda^2}^{m_t^2} \frac{dp_t^2}{(m_t^2 - p_t^2)^{1+2\epsilon}} = -\frac{1}{2\epsilon} + \ln \frac{\Lambda^2}{\mu^2} + \mathcal{O}(\epsilon)$$

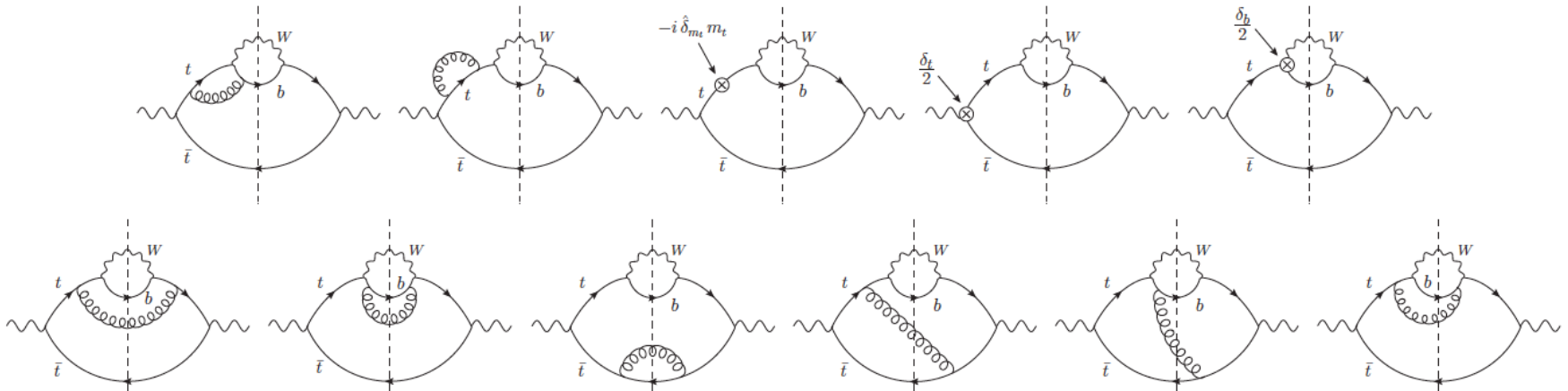
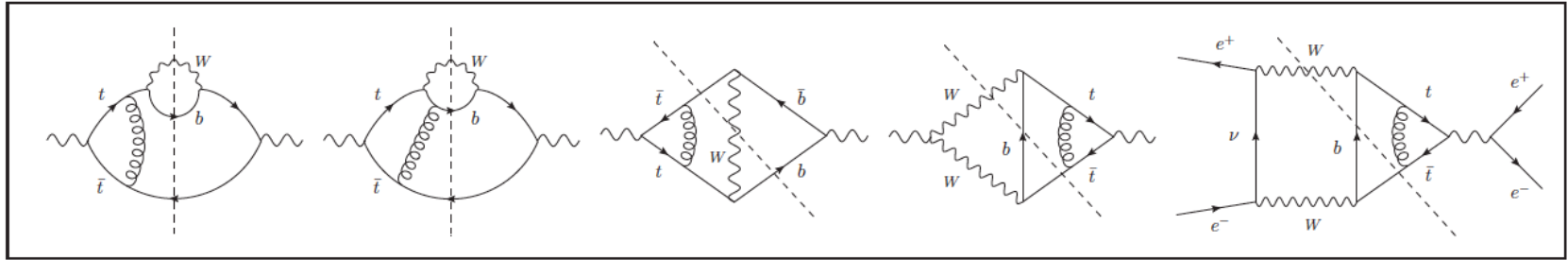
Expand integrand in  $(m_t^2 - p_t^2)/m_t^2 \iff$  asymptotic expansion of result in  $\Lambda/m_t$

# ENDPOINT-DIVERGENT NON-RESONANT NNLO DIAGRAMS

Leading terms in the expansion for  $p_t^2 \rightarrow m_t^2$  of the integrands obtained using the expansion by regions approach

Jantzen, PRF (2013)

~100 diagrams, but only 15% of them contain endpoint divergences



boxed diagrams  $\rightsquigarrow$  endpoint-singular  $\frac{1}{\epsilon} - 2 \ln \frac{\Lambda^2}{\mu^2}$  terms from potential gluons

+ "finite" endpoint-divergent  $\frac{m_t}{\Lambda}$  &  $\frac{m_t^2}{\Lambda^2}$  terms from hard & potential gluons

# Computing non-resonant NNLO contributions

The integrands  $g_{ix}$  of the endpoint divergent contributions regulated dimensionally  $\rightarrow$  loop integrals cannot be expanded in  $d - 4$

Expressions for scalar one-loop integrals in general  $d$ -dim (up to four external legs) are available, but their phase-space integration becomes complicated

Different strategy used: use endpoint divergent terms obtained in [Jantzen, PRF '13](#) as subtractions to the integrands

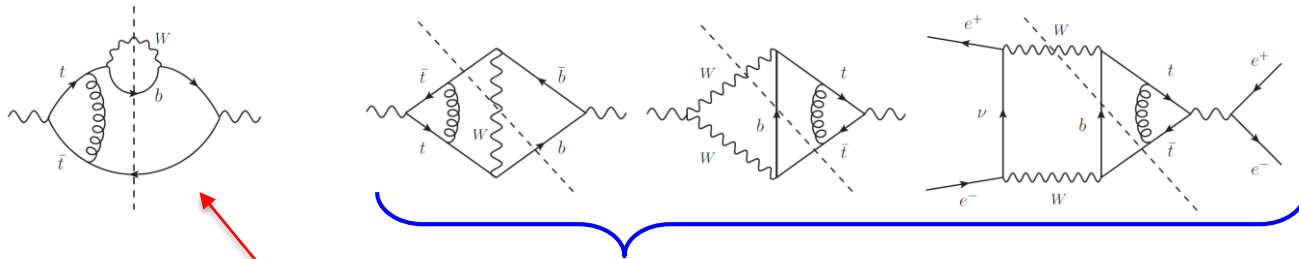
$$t \equiv p_t^2/m_t^2 \quad , \quad y \equiv 1 - \Lambda^2/m_t^2$$

$$\int_y^1 dt g_{ix}(t) = \int_y^1 dt \left[ g_{ix}(t) - \sum_{a=1, \frac{3}{2}, 2} \sum_b \frac{\hat{g}_{ix}^{(a,b)}}{(1-t)^{a+b\epsilon}} \right] + \sum_{a=1, \frac{3}{2}, 2} \sum_b \frac{\hat{g}_{ix}^{(a,b)} (1-y)^{1-a-b\epsilon}}{1-a-b\epsilon}$$

$\mathcal{O}((1-t)^{-\frac{1}{2}}) \rightarrow t$ -integration finite,  
integrand can be expanded in  $\epsilon$

For the rest of contributions (endpoint finite diagrams) we use [MadGraph](#)

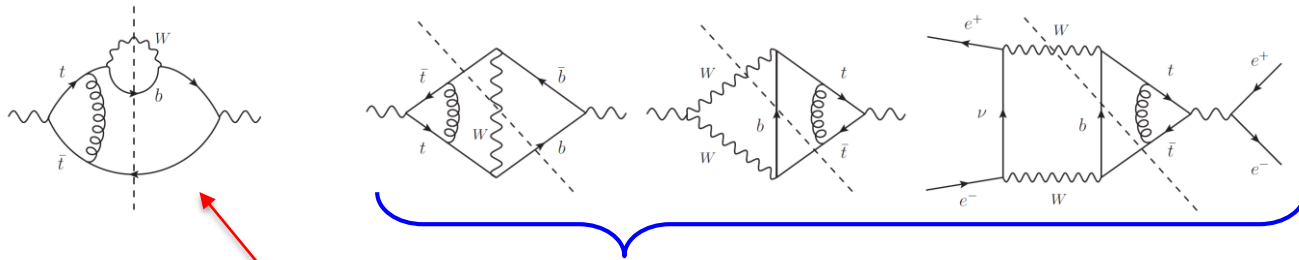
# COMPUTING NON-RESONANT NNLO CONTRIBUTIONS (cont.)



$$\begin{aligned}
 \sigma_{\text{non-res}}^{\text{NNLO}} &= \sigma_{\text{sq}} + \sigma_{\text{int}} + \sigma_{\text{MadG}} \\
 &= \underbrace{\sigma_{\text{sq}} + \sigma_{\text{int}}^{(\text{EPdiv})}}_{\text{UV and IR finite, but endpoint divergent}} + \underbrace{\left[ \sigma_{\text{int}}^{(\text{EPfin})} + \sigma_{\text{MadG}} \right]}_{\text{finite}}
 \end{aligned}$$

→ cancels against  $\frac{\alpha_s \Gamma_t}{\epsilon}$  in resonant part

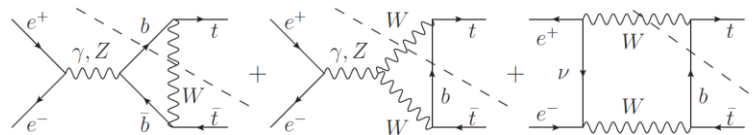
# COMPUTING NON-RESONANT NNLO CONTRIBUTIONS (cont.)



$$\begin{aligned}
 \sigma_{\text{non-res}}^{\text{NNLO}} &= \sigma_{\text{sq}} + \sigma_{\text{int}} + \sigma_{\text{MadG}} \\
 &= \underbrace{\sigma_{\text{sq}} + \sigma_{\text{int}}^{(\text{EPdiv})}}_{\text{UV and IR finite, but endpoint divergent}} + \underbrace{\left[ \sigma_{\text{int}}^{(\text{EPfin})} + \sigma_{\text{MadG}} \right]}_{\text{finite}}
 \end{aligned}$$

→ cancels against  $\frac{\alpha_s \Gamma_t}{\epsilon}$  in resonant part

$$\sigma_{\text{res}}^{\text{NNLO}} = \sigma_{\text{res,rest}} + \sigma_{\text{Abs,bare}}^{(k)}$$



$$\begin{aligned}
 \sigma_{\text{non-res}}^{\text{NNLO}} &= \sigma_{\text{sq}} + \sigma_{\text{int}} + \sigma_{\text{MadG}} \\
 &= \sigma_{\text{sq}} + \sigma_{\text{int}}^{(\text{EPdiv})} + \left[ \sigma_{\text{int}}^{(\text{EPfin})} + \sigma_{\text{MadG}} \right] \\
 \sigma_{\text{res}}^{\text{NNLO}} &= \sigma_{\text{res,rest}} + \sigma_{C_{\text{Abs,bare}}}^{(k)} \\
 &\quad \downarrow \text{part (I)} \qquad \downarrow \text{part (II)} \\
 &\qquad \qquad \qquad \downarrow \text{part (III)}
 \end{aligned}$$

⇒ each of the finite parts can be evaluated in a different computational scheme:

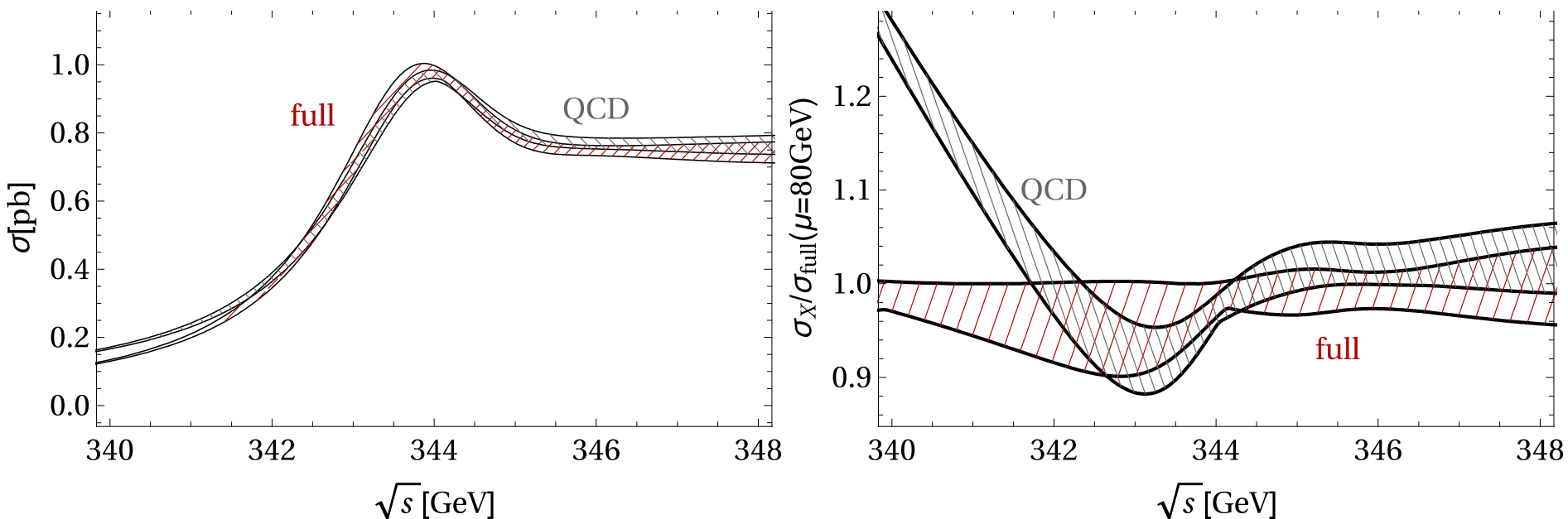
(I): in  $d$ -dim. and NDR scheme for  $\gamma_5$

(II): perform Dirac algebra and inner loop in 4 dim., NDR scheme for  $\gamma_5$

(III): scheme fixed by MadGraph conventions ( $\sigma_{\text{MadG}}$  is UV divergent)

## IV. Results

# Inclusive top-pair production cross section



$$m_t^{\text{PS}} = 171.5 \text{ GeV}$$

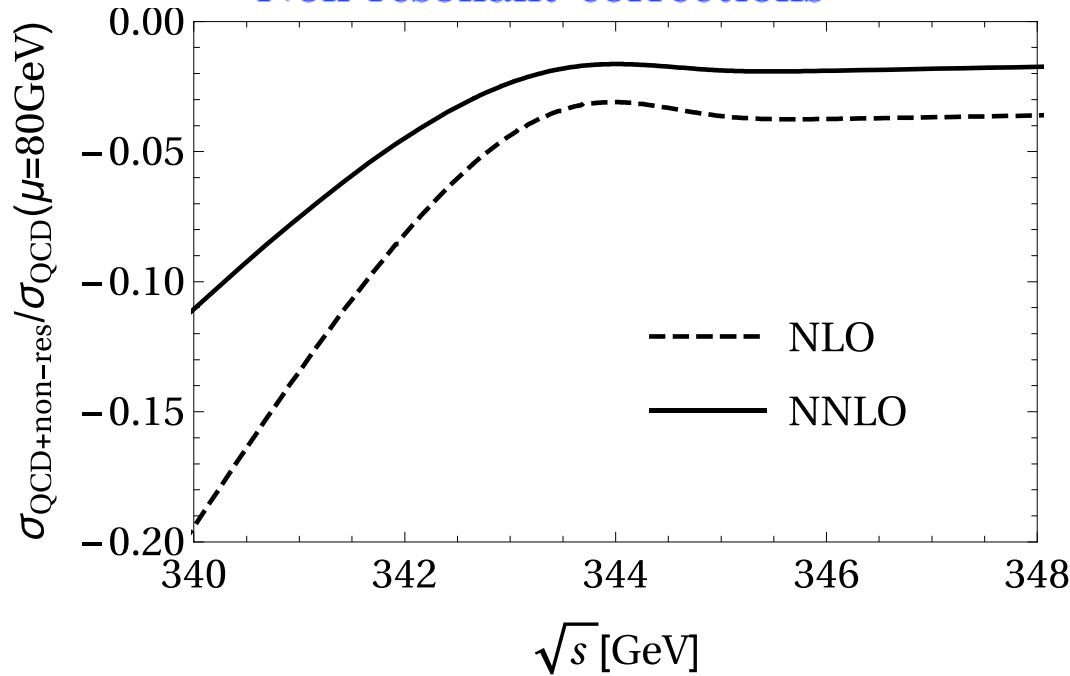
$$\mu_r = 50 - 350 \text{ GeV} \quad (\text{renormalization scale of } \alpha_s)$$

$$\mu_w = 350 \text{ GeV} \quad (\text{scale associated to separation of resonant and nonresonant})$$

- Uncertainty band somewhat increased by EW effects:  $\pm 5\%$  directly below the peak,  $\pm 3\%$  in the rest. Due to Higgs potential insertion [Beneke, Maier, Piclum, Rauh \(2015\)](#)
- Largest effect of EW corrections below the peak, dominated by abs. parts of matching coeffs. and non-resonant

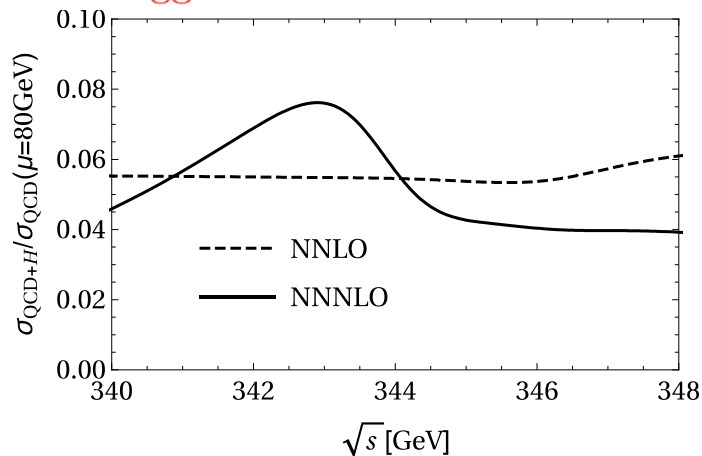
# Size of non-resonant and other non-QCD corrections

## Non-resonant corrections

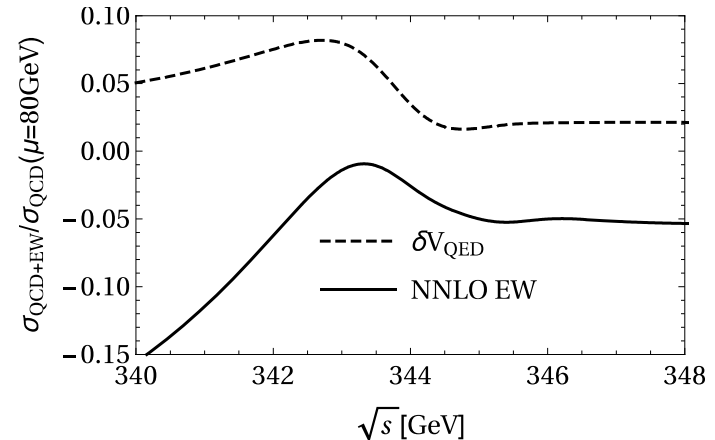


- Nearly energy-independent, shape  $\propto \sigma_{\text{QCD}}^{-1}$
- NLO:  $-(3 - 4)\%$  near and above the peak, up to  $-20\%$  below
- NNLO corrections compensate about half of the NLO result

## Higgs corrections

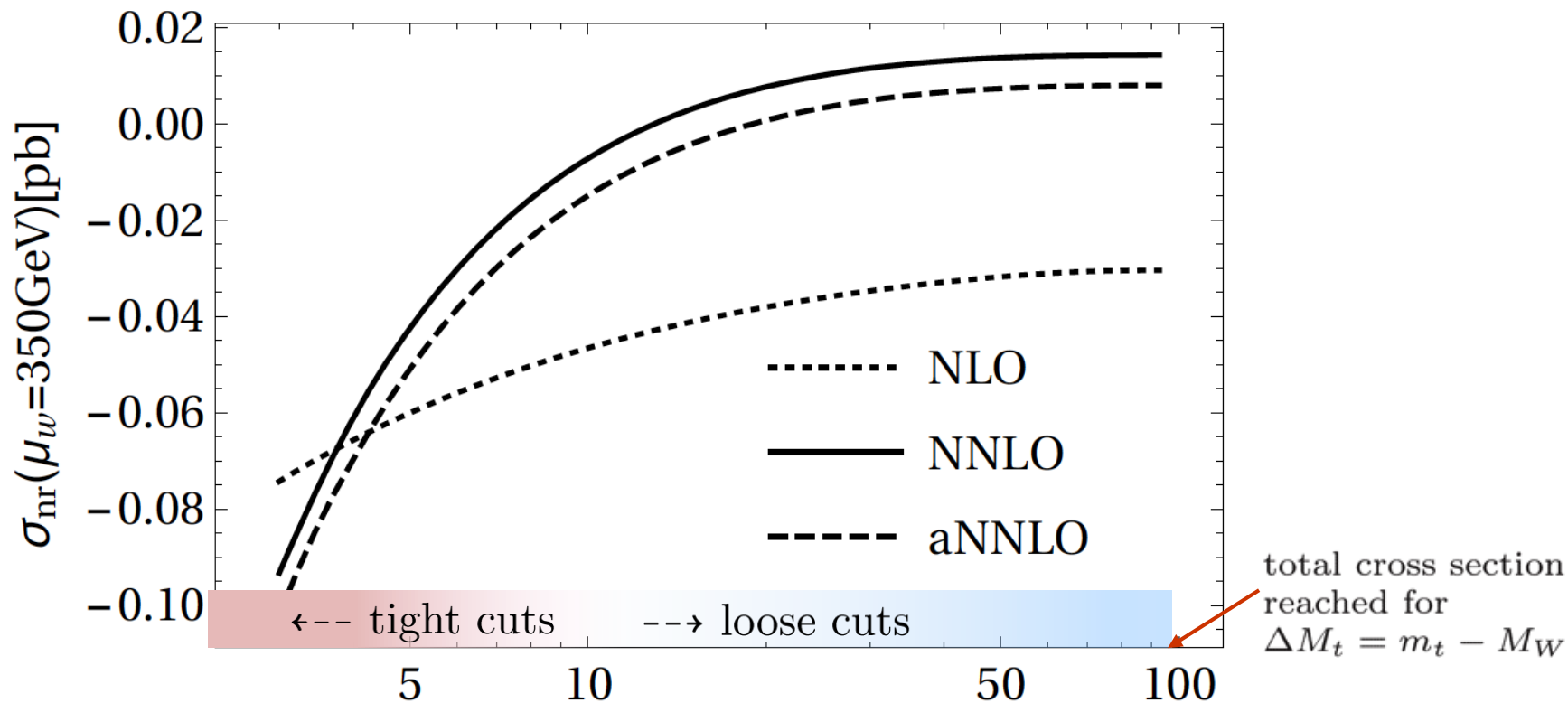


## Other EW corrections



# Non-resonant corrections: dependence on the cut

Cut on  $bW$  invariant masses of the form  $|\sqrt{p_{t,\bar{t}}^2} - m_t| \leq \Delta M_t$



- Tighter cuts increase importance of non-resonant corrections. Resonant contributions unaffected by the cut if  $\Delta M_t \gg \Gamma_t$
- Dashed line: approximate result that includes only the endpoint divergent terms  $\rightarrow m_t^2/\Lambda^2, m_t/\Lambda, \ln(\Lambda/m_t)$  ( $\Lambda^2 \simeq 2m_t\Delta M_t$ )

# V. Summary and outlook

## Non-resonant corrections

- accounts for  $bW$  pairs produced from virtual tops or with only one or no top near the  $t\bar{t}$  threshold
- ✓ **computed at NNLO** for the total cross section and with **top invariant-mass cuts**
- ✓ required to make the QCD prediction consistent (cancellation of finite width divergencies)
- **+2%** effect above threshold, up to **+10%** below the peak; cancels about half of the NLO non-resonant correction
- ✓ **NNLO electroweak accuracy achieved!**

**Outlook:** combine NNNLO with NNLL QCD, incorporate initial state radiation in theory prediction, estimate NNNLO electroweak corrections...

# V. Summary and outlook

## Non-resonant corrections

- accounts for  $bW$  pairs produced from virtual tops or with only one or no top near the  $t\bar{t}$  threshold
- ✓ **computed at NNLO** for the total cross section and with **top invariant-mass cuts**
- ✓ required to make the QCD prediction consistent (cancellation of finite width divergencies)
- **+2%** effect above threshold, up to **+10%** below the peak; cancels about half of the NLO non-resonant correction
- ✓ **NNLO electroweak accuracy achieved!**

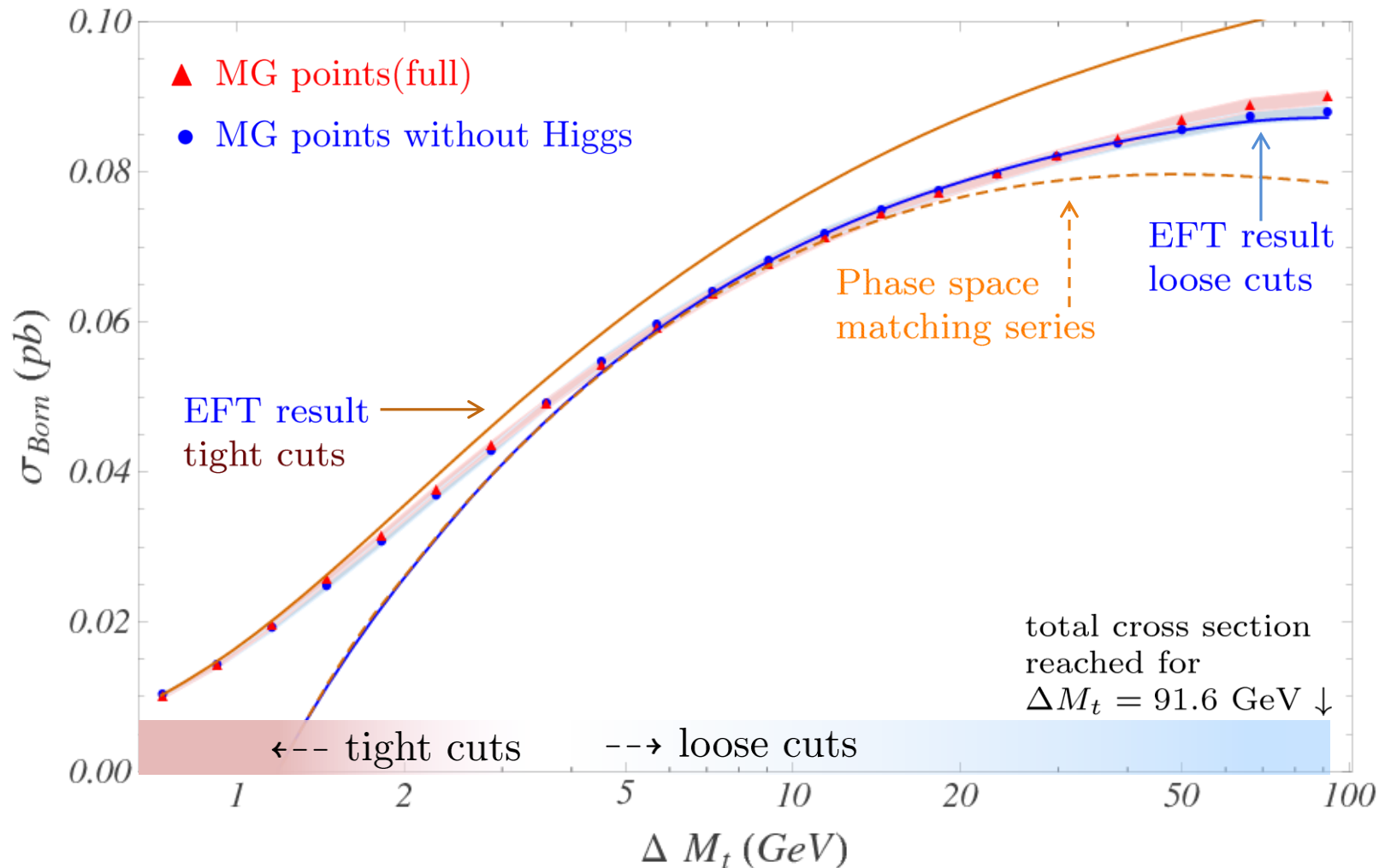
**Outlook:** combine NNNLO with NNLL QCD, incorporate initial state radiation in theory prediction, estimate NNNLO electroweak corrections...

# Thank you!

# Backup slides

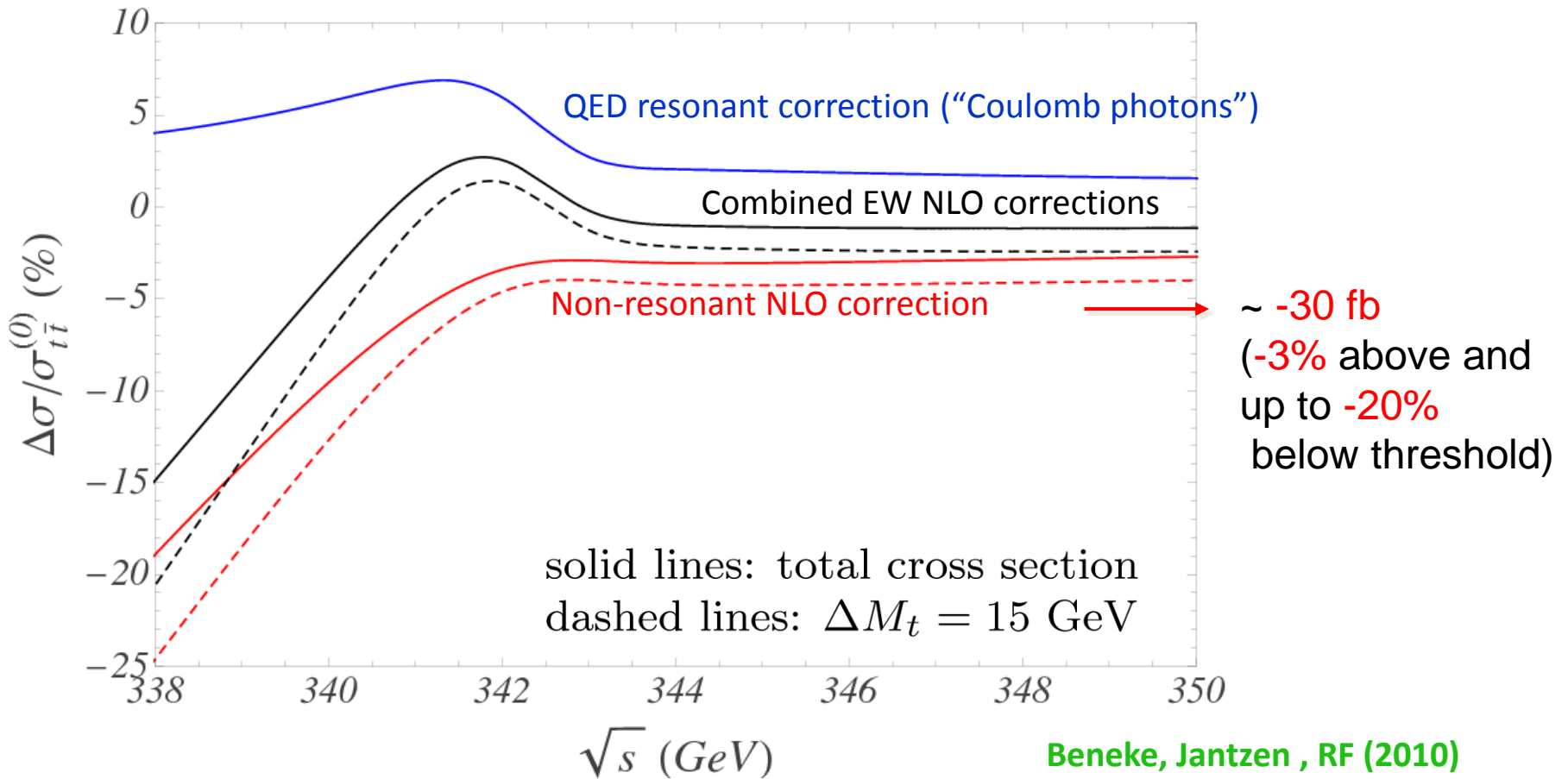
$\hookrightarrow$  generated  $10^4$  events for  $e^+e^- \rightarrow W^+W^-b\bar{b}$  with MadGraph (MG) for  $s = 4m_t^2$ , and analyzed dependence on the  $bW$  invariant-mass cut  $\Delta M_t$

EFT result: resonant LO+NNLO ( $\alpha_s = 0$ ) + non-resonant NLO



# Relative sizes of EW NLO corrections with respect LO

LO includes resummation of Coulomb gluons  $\propto (\alpha_s/v)^n$   $[\alpha_s^{\overline{\text{MS}}}(30 \text{ GeV}) = 0.142]$



# Phase space matching

## Alternative approach to compute non-resonant contributions

Hoang, Reisser, PRF (2010)

- Non-resonant contributions obtained for moderate invariant-mass cuts,  $m_t \Gamma_t \ll \Lambda^2 \ll m_t^2$ , as a series:

$$\frac{\Gamma_t}{\Lambda} \sum_{n,\ell,k} \left[ \left( C(\alpha_s) \times \frac{m_t \Gamma_t}{\Lambda^2} \right)^n \times \left( \frac{\Lambda^2}{m_t^2} \right)^\ell \right] \times \left( \alpha_s \frac{m_t}{\Lambda} \right)^k \quad n, \ell, k = 0, 1, \dots$$

- NLO, NNLO and (partial) N<sup>3</sup>LO contributions obtained (counting  $\Lambda \sim m_t$ ) ✓
- Beyond NLO, phase space matching approach cannot be applied to larger cuts up to the total cross section ✗
- Expansion of full NLO non-resonant contributions in  $(\Lambda/m_t)^n$  agrees with first two terms in series above  
[higher powers receive contributions from diagrams h5-h10 with no top, not taken into account in the psm approach → remainder contributions, small at NLO ✓ ]

# Non-resonant NNLO contribution for total cross section

Alternative framework [Penin, Piclum, 2012] computes non-resonant contributions to the total cross section by expanding in

$$\rho = 1 - M_W/m_t \approx 0.5$$

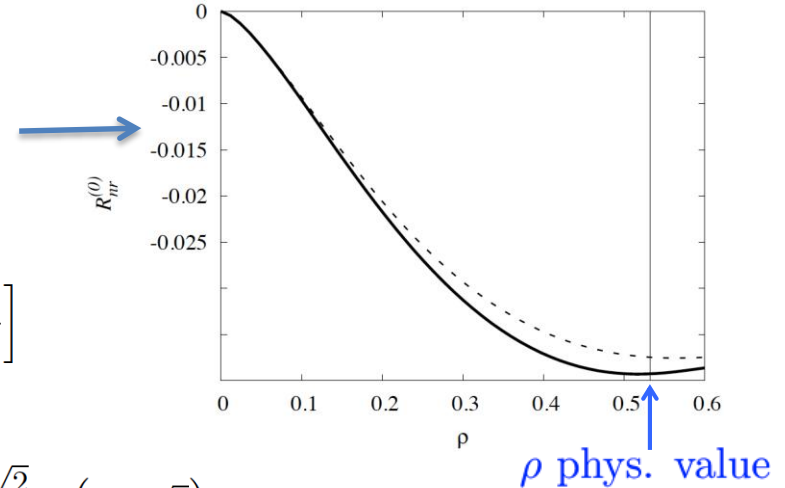
- at NLO, the first term in  $\rho$  deviates from the exact result by less than 5%

- at NNLO

$$R_{nr}^{(1)} = \frac{N_c C_F \alpha_s}{\pi^2 \rho} \frac{\Gamma_t}{m_t} \left\{ \left[ Q_e^2 Q_t^2 + \frac{2Q_e Q_t v_e v_t}{1-x_Z} + \frac{(a_e^2 + v_e^2)v_t^2}{(1-x_Z)^2} \right] \times \left[ (3L_E + \frac{3}{2} + 6\ln 2) \pi^2 + (18 + 24\ln 2) \rho^{1/2} \right] + \frac{1}{s_w^4} \left[ \frac{22}{3} + \frac{17\pi^2}{6} - \frac{17}{2} \ln 2 + (2 - 3\pi^2 + 9\ln 2) \frac{3\sqrt{2}}{4} \ln(1 + \sqrt{2}) - \frac{27\sqrt{2}}{8} (\ln^2(1 + \sqrt{2}) + \text{Li}_2(2\sqrt{2} - 2)) \right] \rho^{1/2} + \mathcal{O}(\rho) \right\}.$$

$L_E = \ln\left(\frac{\sqrt{E^2 + \Gamma_t^2}}{\rho m_t}\right) \rightarrow$  infrared regularization dependent term. But dim. reg. used for the resonant contributions, not clear how to combine both

Moreover: infrared structure does not agree with that our (exact in  $\rho$ ) result  $\rightarrow$  diagram missing in this computation



# Endpoint-divergent non-resonant NNLO contribution

↪ **dominant contribution for small  $\Lambda$**  (or small  $\Delta M_t$ )

$$\sigma_{\text{non-res}}^{(2),\text{ep}} = \frac{64\pi^2 \alpha^2}{s} \frac{\Gamma_t^{\text{Born}}}{m_t} \left[ C_{\dots}(s) = \gamma/Z\text{-prop. \& } e^\pm\text{-coupl.} \right]$$

$$\times \left\{ \left[ Q_t^2 C_{\gamma\gamma}(s) - 2Q_t v_t C_{\gamma Z}(s) + v_t^2 C_{ZZ}(s) \right] \left\{ 4N_c C_F \frac{\alpha_s}{\pi} \frac{m_t^2}{\Lambda^2} + \frac{6\sqrt{2}}{\pi^2} \left( \delta\Gamma_t^{(1)} - \frac{4C_F}{\pi} \alpha_s \right) \frac{m_t}{\Lambda} \right\} \right.$$

$$+ N_c C_F \frac{\alpha_s}{4\pi} \left( \frac{1}{\epsilon_{\text{ep}}} + 2 \ln \frac{\mu_s^2}{\Lambda^2} \right) \left\{ \left[ Q_t^2 C_{\gamma\gamma}(s) - 2Q_t v_t C_{\gamma Z}(s) + v_t^2 C_{ZZ}(s) \right] \frac{7 + 7x + 22x^2}{6(x-1)(1+2x)} \right.$$

$$+ \frac{1}{3} a_t^2 C_{ZZ}(s) + \frac{1}{2} Q_t a_t C_{\gamma Z}(s) - \frac{1}{2} v_t a_t C_{ZZ}(s)$$

$$+ \left[ Q_t Q_b C_{\gamma\gamma}(s) - (Q_t (v_b + a_b) + Q_b v_t) C_{\gamma Z}(s) + v_t (v_b + a_b) C_{ZZ}(s) \right] \frac{1 - 5x - 2x^2}{6(1+x)(1+2x)}$$

$$+ \left[ Q_t C_{\gamma\gamma}(s) - \left( v_t + Q_t \frac{c_w}{s_w} \right) C_{\gamma Z}(s) + v_t \frac{c_w}{s_w} C_{ZZ}(s) \right] \frac{2 + 5x - 2x^2}{6x(1+2x)}$$

$$\left. - \left[ Q_t C_\gamma(s) + v_t C_Z(s) \right] \left[ \ln \left( \frac{2}{x} - 1 \right) + \frac{(1-x)(1-2x-23x^2)}{12x^2} \right] \frac{x}{4(1-x)^3(1+2x)} \right\} \left. \right\}$$

+ **finite  $\Lambda$ -independent terms** +  $\mathcal{O}(\Lambda/m_t)$

**Jantzen, PRF (2013)**

- UV and IR singularities cancelled between diagrams ✓
- **$1/\epsilon$  endpoint singularities & finite-width divergences** cancel each other ✓
- comparison to HRR result:  $m_t^2/\Lambda^2$  ✓,  $m_t/\Lambda$  ✓,  $\Lambda^0 \ln(\Lambda^2)$  ✓